

See discussions, stats, and author profiles for this publication at: <https://www.researchgate.net/publication/23290198>

# Compact optical temporal differentiator based on silicon microring resonator

Article in *Optics Express* · October 2008

DOI: 10.1364/OE.16.015880 · Source: PubMed

CITATIONS

156

READS

982

7 authors, including:



**Tong Ye**

Shanghai Jiao Tong University

99 PUBLICATIONS 836 CITATIONS

[SEE PROFILE](#)



**Ziyang Zhang**

Westlake University

136 PUBLICATIONS 3,264 CITATIONS

[SEE PROFILE](#)



**Min Qiu**

Zhejiang University

368 PUBLICATIONS 10,821 CITATIONS

[SEE PROFILE](#)

Some of the authors of this publication are also working on these related projects:



microring-based modulator [View project](#)



ICT-POLYSYS [View project](#)

# Compact optical temporal differentiator based on silicon microring resonator

Fangfei Liu,<sup>1</sup> Tao Wang,<sup>1</sup> Li Qiang,<sup>1</sup> Tong Ye,<sup>1</sup> Ziyang Zhang,<sup>2</sup> Min Qiu,<sup>2</sup> and Yikai Su<sup>1,\*</sup>

<sup>1</sup>State Key Lab of Advanced Optical Communication Systems and Networks, Department of Electronic Engineering, Shanghai Jiao Tong University, 800 Dongchuan Rd, Shanghai 200240, China

<sup>2</sup>Department of Microelectronics and Applied Physics, Royal Institute of Technology, Electrum 229, 164 40 Kista, Sweden

\*Corresponding author: [yikaisu@sjtu.edu.cn](mailto:yikaisu@sjtu.edu.cn)

**Abstract:** We propose and experimentally demonstrate a temporal differentiator in optical field based on a silicon microring resonator with a radius of 40  $\mu\text{m}$ . The microring resonator operates near the critical coupling region, and can take the first order derivative of the optical field. It features compact size thus is suitable for integration with silicon-on-insulator (SOI) based optical and electronic devices. The performance of this optical differentiator is tested using signals with typical shapes such as Gaussian, sinusoidal and square-like pulses at data rates of 10 Gb/s and 5 Gb/s.

©2008 Optical Society of America

**OCIS codes:** (130.7408) Wavelength filtering devices; (200.3050) Information processing; (200.4560) Optical data processing; (230.1150) All-optical devices.

---

## References and links

1. N. K. Berger, B. Levit, B. Fischer, M. Kulishov, D. V. Plant, and J. Azaña, "Temporal differentiation of optical signals using a phase-shifted fiber Bragg grating," *Opt. Express* **15**, 371-381 (2007), <http://www.opticsinfobase.org/abstract.cfm?URI=oe-15-2-371>.
2. J. Xu, X. Zhang, J. Dong, D. Liu, and D. Huang, "All-optical differentiator based on cross-gain modulation in semiconductor optical amplifier," *Opt. Lett.* **32**, 3029-3031 (2007), <http://www.opticsinfobase.org/abstract.cfm?URI=ol-32-20-3029>.
3. N. Q. Ngo, S. F. Yu, S. C. Tjin, and C. H. Kam, "A new theoretical basis of higher-derivative optical differentiators," *Opt. Commun.* **230**, 115-129 (2004).
4. Z. Li, S. Zhang, J. M. Vazquez, Y. Liu, G. D. Khoe, H. J. S. Dorren, and D. Lenstra, "Ultrafast optical differentiators based on asymmetric Mach-Zehnder interferometer," presented at the Symposium of the IEEE/LEOS, Benelux Chapter (2006).
5. G. Lenz, B. J. Eggleton, C. K. Madsen, and R. E. Slusher, "Optical delay lines based on optical filters," *IEEE J. Quantum Electron.* **37**, 525-532 (2001).
6. G. S. Pandian and F. E. Seraji, "Optical pulse response of a fiber ring resonator," *IEEE Proceedings-J*, **138**, 235-239 (1991).
7. L. Li, X. Zhang, P. Sun, and L. Chen, "Microring resonator-coupled Mach-Zehnder interferometer as trigger pulse generator, optical differentiator and integrator," *Fundamental Problems of Optoelectronics and Microelectronics III, Proceedings of the SPIE*, **6595**, 659513-1-659513-8 (2007).
8. R. Slavík, Y. Park, M. Kulishov, R. Morandotti, and J. Azaña, "Ultrafast all-optical differentiators," *Opt. Express* **14**, 10699-10707 (2006), <http://www.opticsinfobase.org/abstract.cfm?URI=oe-14-22-10699>.
9. Q. Xu, V. R. Almeida, and M. Lipson, "Micrometer-scale all-optical wavelength converter on silicon," *Opt. Lett.* **30**, 2733-2735 (2005), <http://www.opticsinfobase.org/abstract.cfm?URI=ol-30-20-2733>.
10. Z. Zhang, M. Dainese, L. Wosinski, and M. Qiu, "Resonance-splitting and enhanced notch depth in SOI ring resonators with mutual mode coupling," *Opt. Express* **16**, 4621-4630 (2008), <http://www.opticsinfobase.org/abstract.cfm?URI=oe-16-7-4621>.
11. S. Scheerlinck, J. Schrauwen, F. Van Laere, D. Taillaert, D. Van Thourhout, and R. Baets, "Efficient, broadband and compact metal grating couplers for silicon-on-insulator waveguides," *Opt. Express* **15**, 9639-9644 (2007), <http://www.opticsinfobase.org/viewmedia.cfm?uri=oe-15-15-9625&seq=0>.
12. F. Liu, Q. Li, Z. Zhang, M. Qiu, and Y. Su, "Optically tunable delay line in silicon microring resonator based on thermal nonlinear effect," *IEEE J. Sel. Top. Quantum Electron.* **14**, 706-712 (2008).
13. A. V. Oppenheim, A. S. Willsky, and S. H. Nawab, *Signals and Systems*, 2nd ed. (Prentice Hall, 1996), ch. 4.
14. G. Roelkens, D. Vermeulen, D. Van Thourhout, R. Baets, S. Brision, P. Lyan, P. Gautier, and J.-M. Fedeli, "High efficiency SOI fiber-to-waveguide grating couplers fabricated using CMOS technology," in

## 1. Introduction

All-optical signal processing technology is a promising solution to overcome the speed bottleneck of the electronic devices. A general goal of this technology is to design and implement the equivalent devices in photonics to those in electronics [1]. Optical temporal differentiator, which takes the time derivative of the complex optical field, is one of the building blocks for all-optical signal processing. It can find applications in many areas such as optical processing of microwave signals [1], analog-digital conversion [2], pulse shaping [2], and dark-soliton detection [3].

Several methods have been proposed to realize the optical differentiator. Some are based on the transversal filter structure [3] or the asymmetric Mach-Zehnder interferometer [4], which can be synthesized using planar lightwave circuit (PLC) technology. However, these schemes are only studied theoretically; also, they belong to the finite impulse response (FIR) filters which exhibit relatively large physical lengths of the devices [5]. Ref. [6] and [7] investigate the differentiation function of a fiber ring resonator and microring resonator-coupled Mach-Zehnder interferometer at the theory level. Other works include experimental demonstrations of fiber-based devices as optical differentiators such as long period fiber grating (LPG) [8] and phase-shifted fiber Bragg grating [1]. The LPG can process signals as fast as 180 fs with a length in the order of several centimeters, and the phase-shifted fiber Bragg grating shows high efficiency in processing signals of bandwidths up to a few GHz with a device length of 1 mm. To the best of our knowledge, no experimental demonstration has been performed with compact, integrated optical differentiator on chip.

Recently, silicon photonics has received intensive interests as the silicon-on-insulator (SOI) structure is considered as a candidate platform for photonic integrated circuits due to its compact size and compatibility with electronics [9]. In this paper, we propose an optical temporal differentiator based on a silicon microring resonator and investigate the performance of the optical differentiator. We fabricate a compact silicon microring resonator with a radius of 40  $\mu\text{m}$  and experimentally test its differentiation performance using signals with typical shapes such as Gaussian, sinusoidal and square-like pulses at data rates of 10 Gb/s and 5 Gb/s.

## 2. Operating principle

An optical temporal differentiator which takes the first derivative of the optical field in the time domain can provide the transfer function of the form  $T(\omega) = j(\omega - \omega_0)$  in the frequency domain, where  $\omega_0$  is the optical carrier frequency [1]. This transfer function shows that the transmission of the differentiator is linearly dependent on the frequency detuning from the central frequency and the phase response has an exact  $\pi$  phase-shift across the central frequency. Here we demonstrate that the transfer function of a single side coupled silicon microring resonator operating at the critical coupling region is a good approximation to that of a temporal differentiator.

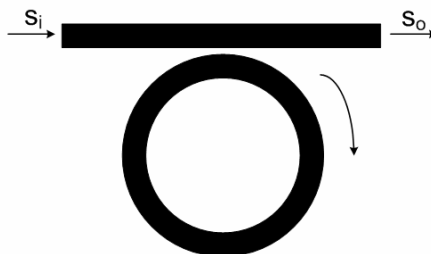


Fig. 1. Schematic of a microring resonator

The basic structure of the silicon microring resonator used in the experiment is a ring evanescently coupled to a single straight waveguide as shown in Fig. 1. According to the coupled mode theory, the transfer function of the microring resonator can be expressed as [10]:

$$T(\omega) = \frac{s_0}{s_i} = \frac{j(\omega - \omega_0) + \frac{1}{\tau_i} - \frac{1}{\tau_e}}{j(\omega - \omega_0) + \frac{1}{\tau_i} + \frac{1}{\tau_e}} \quad (1)$$

where  $\omega_0$  is the resonance frequency,  $1/\tau_i$  is the power decay rate due to the intrinsic loss and  $1/\tau_e$  is the power coupling to the waveguide, which are related to the reciprocal of photon lifetime as  $1/\tau = 1/\tau_i + 1/\tau_e$ . Under the condition that the frequency detuning is much less than the 3-dB bandwidth of the resonator, the expression can be approximated as:

$$T(\omega) = j\tau(\omega - \omega_0) + \frac{\frac{1}{\tau_i} - \frac{1}{\tau_e}}{\frac{1}{\tau_i} + \frac{1}{\tau_e}} \quad (2)$$

This equation means that a single coupled microring resonator can be modeled as a differentiator with certain gain plus a constant-output. In particular, when the microring resonator works in the critical coupling region ( $\tau_e = \tau_i$ ), we obtain:

$$T(\omega) = j\tau(\omega - \omega_0) \quad (3)$$

which is a typical function for a first-order temporal differentiator. Figure 2 shows the transmission and phase response for a microring resonator operating at and close to the critical coupling region, respectively. The parameters used in simulations are identical to those in the experiment for comparison. The phase response in Fig. 2(a) has an exact  $\pi$  phase-shift across the central frequency while the phase jump at the central frequency in Fig. 2(b) is not abrupt, which is the case for a practical device.

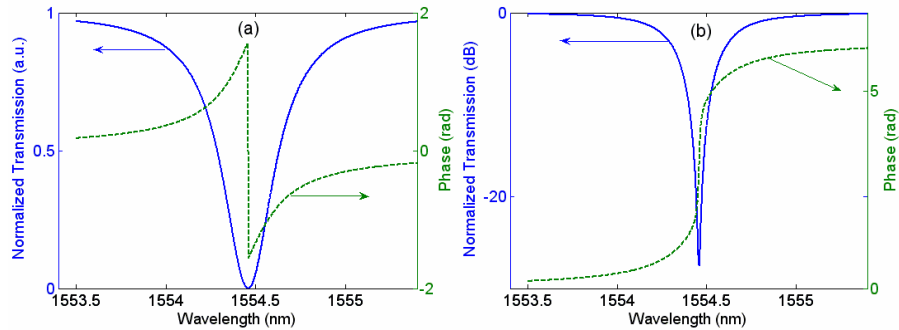


Fig. 2. Transmission and phase response of microring resonator operating (a) at the critical coupling, (b) close to the critical coupling region.

### 3. Device fabrication

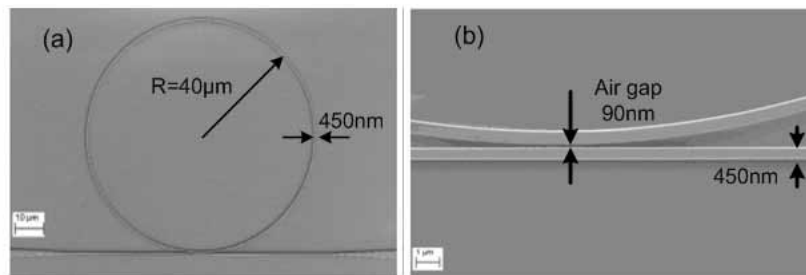


Fig. 3. (a) SEM photo of the microring resonator, (b) zoom-in view of the coupling region.

In order to achieve the critical coupling, we fabricated a set of silicon microring resonators with radius of 40  $\mu\text{m}$  on a SOI wafer and varied the air gap between the waveguide and the ring from 80 nm to 150 nm in small steps (10 nm). We find that the structure with an air gap of  $\sim 90$  nm gives the deepest notch, which indicates the approach of critical coupling. The cross section of the silicon waveguide is  $450 \times 250$  nm on top of a 3- $\mu\text{m}$  silica buffer layer to prevent optical mode from leaking to the substrate. The device is fabricated by E-beam lithography followed by reactive ion etching. The surface roughness is reduced by oxidizing 20 Å of silicon surfaces using wet chemistry. The scanning electron microscope (SEM) photo of the silicon microring resonator is shown in Fig. 3. The measured and fitted transmission spectra of the microring resonator are depicted in Fig. 4. The notch depth at the resonance is  $\sim 27$  dB, implying that the resonator is very close to the critical coupling. The 3-dB bandwidth of the resonator is  $\sim 0.34$  nm for the resonance at  $\sim 1554.46$  nm, which is large enough for signal processing at a data rate of 10 Gb/s.

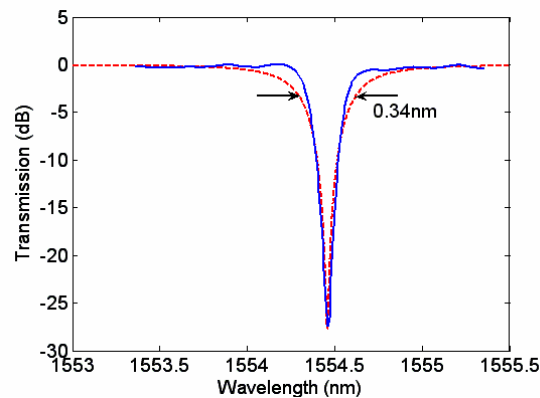


Fig. 4. Measured (solid) and fitted (dashed) spectrum of the resonance at 1554.46 nm.

#### 4. Experimental setup

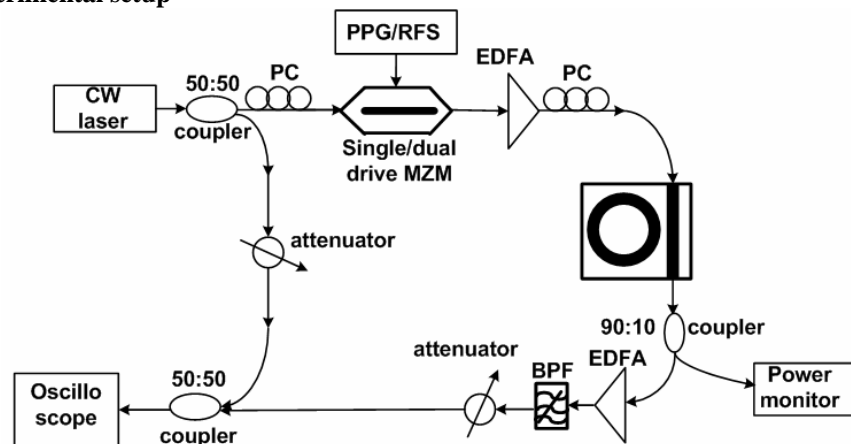


Fig. 5. Experimental setup for testing the performance of the microring-resonator based optical differentiator. BPF: bandpass filter.

We use the experimental setup shown in Fig. 5 to test the performance of the fabricated microring resonator as an optical differentiator. The desired pulse shape is generated by driving a Mach-Zehnder modulator (MZM) using the pulse pattern generator (PPG) or a radio frequency synthesizer (RFS). When the MZM is biased at the quadrature point of the transmission curve and driven by an electronic square pulse and sinusoidal signal, respectively, we obtain optical square pulse and Gaussian-like pulse (50%-duty-cycle) accordingly. When

the MZM is biased at the transmission null and driven by the electronic sinusoidal signal, the generated signal is a 67%-duty-cycle carrier-suppressed return-to-zero (CS-RZ) signal, which possesses the similar property as the sinusoidal signal in the optical field. To observe the pulse before and after differentiation in the optical field domain, we mix the signal pulse and a continuous wave (CW) light on the same wavelength as the signal before sending it to an oscilloscope. We use vertical coupling to couple light between the fiber and the silicon waveguide [11] as shown in Fig. 6. As the fiber-to-fiber coupling loss of the vertical coupling is  $\sim 20$  dB [12], the signal pulse is amplified using two Erbium-doped fiber amplifiers (EDFAs) before and after the microring resonator, respectively. Meanwhile, the gold grating coupler for vertical coupling is polarization-dependent, a polarization controller (PC) is inserted before the silicon microring resonator to make sure that the input light is transverse electrical (TE) mode.

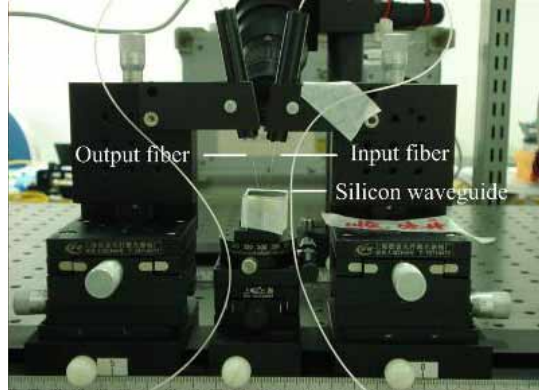


Fig. 6. Picture of the vertical coupling system.

## 5. Experimental results

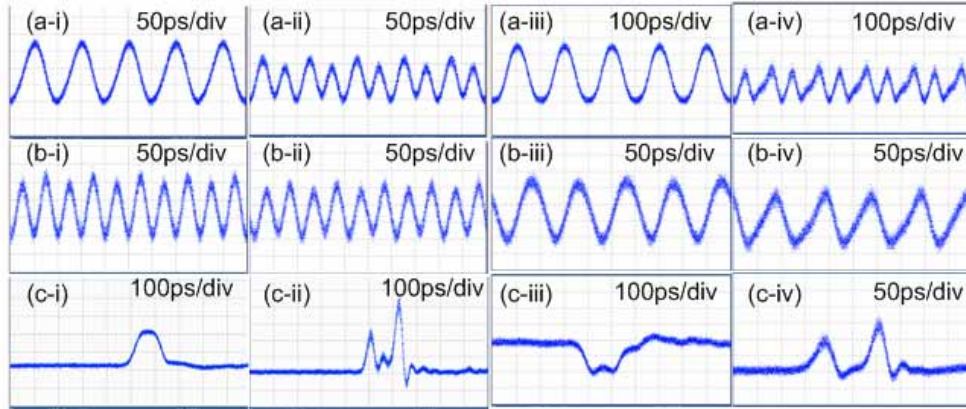


Fig. 7. (a-i) 10-Gb/s and (a-iii) 5-Gb/s input Gaussian-like pulses; (a-ii) 10-Gb/s and (a-iv) 5-Gb/s output OS-HG pulses; (b-i) 10-Gb/s and (b-iii) 5-Gb/s input sinusoidal-like pulses; (b-ii) 10-Gb/s and (b-iv) 5-Gb/s output sinusoidal-like pulse; 10-Gb/s (c-i) single '1' and (c-iii) single '0' input square pulse; differentiation results of 10-Gb/s (c-ii) single '1' and (c-iv) single '0' square pulse.

Figure 7 shows the differentiation results of the Gaussian and sinusoidal-like pulses at data rates of 10 Gb/s and 5 Gb/s, as well as 10-Gb/s square pulses with a pattern of single '1' followed by 15 '0' and single '0' followed by 15 '1'. Theoretically, when the input of the optical differentiator is Gaussian pulses, the output is odd-symmetry Hermite-Gaussian pulses (OS-HG) [8] which are symmetric in intensity and odd-symmetric in the optical field; For the sinusoidal pulses, the output of the differentiator is still sinusoidal pulses and the



differentiation of a square pulse results in two impulses at the rising and falling edges [13]. Figure 8 provides the theoretical and experimental traces for the differentiation of three types of input signals at data rate of 10 Gb/s. As the input signal in the experiment is hard to reproduce in the simulations due to the imperfections of the electrical driving signal and the Mach-Zehnder modulator (MZM), we assume an ideal electrical driving signal and MZM in the simulations. Comparing the theoretical and experimental traces, the two curves have nearly the same shapes. For the Gaussian-like and square pulses, the asymmetry of the two lobes in the experiments is induced by the third order dispersion of the microring-resonator at the resonance wavelength [12], and slight asymmetry of the input signal itself. The broadening of the pulses comes from the limited bandwidth of the MZM in generating the 10-Gb/s signals and the response of the detector in the oscilloscope. Note that the negative intensity in the experimental curve of square pulse is due to the response of the oscilloscope.

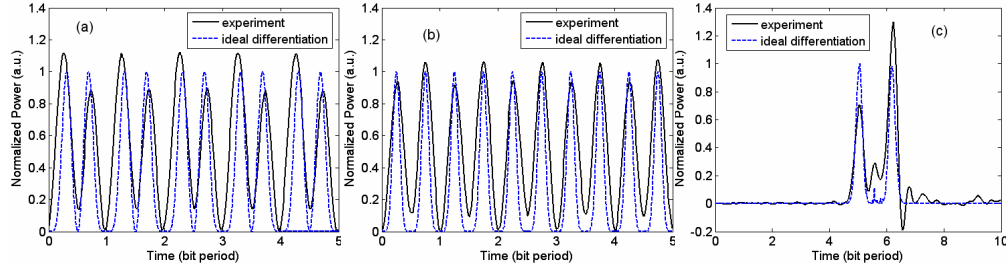


Fig. 8. Theoretical (dashed) and experimental (solid) traces of the differentiation of 10-Gb/s input (a) Gaussian-like, (b) sinusoidal-like, (c) square signals, respectively

In addition, by comparing the differentiation results of the 5-Gb/s and 10-Gb/s Gaussian and sinusoidal-like pulses, there is not much degradation for processing signal with relatively low data rate. Figure 9 provides the waveforms of the 10-Gb/s Gaussian and sinusoidal-like pulse and their first derivative after mixing with the CW light. The oscilloscope can only show the envelope of the mixed signal because the relative phase between the signal and the coherent CW light drifts due to different path lengths; However, unlike the input Gaussian pulse, the polarity between two lobes of the OS-HG pulse changes as in the sinusoidal pulse case. These experiments with the three signals clearly demonstrate all-optical differentiation functionality in the field using this compact silicon device.

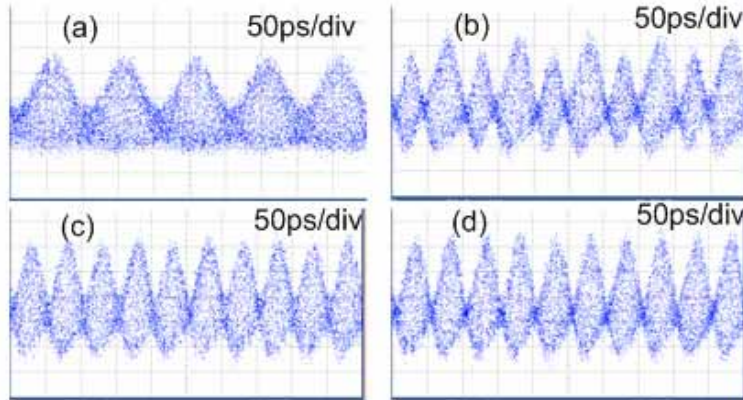


Fig. 9. Waveforms after mixing with the CW light for (a), (b) Gaussian-like pulses; (c), (d) sinusoidal-like pulses before and after differentiation at the data rate of 10 Gb/s, respectively.

Compared with the state-of-the-art solution [1], our device has nearly the same processing bandwidth as that in Ref. [1]; the efficiency of the differentiator in processing 10 Gb/s Gaussian-like pulses is  $\sim 5\%$ , which is comparable with the result in Ref. [1] ( $\sim 3\%$ ). The asymmetry of the waveform induced by the third order dispersion at resonance

wavelength of the microring resonator with finite transmission notch depth is a critical factor affecting the accuracy of the microring resonator based differentiator. This asymmetry almost disappears when reaching the critical coupling operation. The accuracy of our device is relatively lower than Ref. [1], however, this imperfection can be overcome by further increasing the notch depth of the transmission of the microring resonator to approach the critical coupling condition. The coupling loss between the fiber and silicon microwaveguide is ~10 dB, this is not a major limitation in our experiment. Furthermore, the coupling loss could be reduced to ~ 1 dB if optimized grating coupler structures are used [14].

## **6. Conclusion**

We have proposed and demonstrated an optical differentiator based on silicon microring resonator. The performance of the differentiator is experimentally tested with three typical signals: Square, Gaussian-like, and sinusoidal-like pulses, showing the effectiveness of the compact optical differentiator.

## **Acknowledgments**

This work was supported by the NSFC (60777040), Shanghai Rising Star Program Phase II (07QH14008), Swedish Foundation for Strategic Research (SSF), and the Swedish Research Council (VR).